Homogenization of an ensemble of interacting resonant scatterers

N. J Schilder, Christophe Sauvan, Yvan R. P. Sortais, Antoine Browaeys, J.-J. Greffet

Homogenization of an ensemble of interacting resonant scatterers

N. J. Schilder, C. Sauvan, Y. R. P. Sortais, A. Browaeys, and J.-J. Greffet
Laboratoire Charles Fabry, Institut d'Optique Graduate School, CNRS, Université Paris-Saclay, 91127 Palaiseau Cedex, France
(Received 4 June 2017; published 13 July 2017)

We study theoretically the concept of homogenization in optics using an ensemble of randomly distributed resonant stationary atoms with density ρ. The ensemble is dense enough for the usual condition for homogenization, viz. $\rho\lambda^3 \gg 1$, to be reached. Introducing the coherent and incoherent scattered powers, we define two criteria to define the homogenization regime. We find that when the excitation field is tuned in a broad frequency range around the resonance, neither of the criteria for homogenization is fulfilled, meaning that the condition $\rho\lambda^3 \gg 1$ is not sufficient to characterize the homogenized regime around the atomic resonance. We interpret these results as a consequence of the light-induced dipole-dipole interactions between the atoms, which implies a description of scattering in terms of collective modes rather than as a sequence of individual scattering events. Finally, we show that, although homogenization can never be reached for a dense ensemble of randomly positioned laser-cooled atoms around resonance, it becomes possible if one introduces spatial correlations in the positions of the atoms or nonradiative losses, such as would be the case for organic molecules or quantum dots coupled to a phonon bath.

DOI: 10.1103/PhysRevA.96.013825

I. INTRODUCTION

Homogenization is the procedure by which one replaces a discrete distribution of particles by a continuous density distribution. In the framework of the electrodynamics of continuous media, the standard procedure of homogenization, described in many textbooks [1–3], supposes that the interparticle distance $\rho^{-\frac{1}{3}}$ (ρ is the spatial density) is much smaller than the characteristic length scale associated with the phenomenon under study, usually the propagation of a wave through the medium. The characteristic scale being the wavelength λ, the condition for homogenization is thus assumed to be $\rho\lambda^3 \gg 1$. When this condition is satisfied, one derives the *macroscopic* properties of an ensemble of scatterers from the *microscopic* properties of each of them by means of an effective medium theory. In the context of optics, for example, several models exist that relate the (microscopic) atomic polarizability [4] or the dielectric constants of spherical nanoparticles in a composite dielectric random medium [5–10] to the (macroscopic or effective) dielectric constant of the system.

To derive criteria for homogenization in optics, one usually decomposes the electric field scattered by an ensemble of scatterers (e.g., atoms) into coherent and incoherent (or diffuse) components, $\langle \mathbf{E}_{\rm sc}\rangle$ and $\delta\mathbf{E}_{\rm sc}$, respectively: $\mathbf{E}_{\rm sc} = \langle \mathbf{E}_{\rm sc}\rangle + \delta\mathbf{E}_{\rm sc}$, where $\langle \delta\mathbf{E}_{\rm sc}\rangle = 0$. Here $\langle . \rangle$ denotes an ensemble average over many different spatial realizations. The *coherent* (or average) monochromatic field $\langle \mathbf{E}_{\rm sc}\rangle$ follows the Helmholtz equation with an effective (i.e., ensemble-averaged) dielectric constant $\epsilon_{\rm eff}(\omega,\mathbf{r})$ describing the medium [4,7–9]:

$$\boldsymbol{\nabla} \times \boldsymbol{\nabla} \times \langle \mathbf{E}_{\rm sc}\rangle - \epsilon_{\rm eff}(\omega,\mathbf{r})\frac{\omega^2}{c^2}\langle \mathbf{E}_{\rm sc}\rangle = 0. \qquad (1)$$

Importantly, one can always associate an effective dielectric constant (and therefore an effective index of refraction) to this coherent component, no matter whether the medium is homogeneous or not, and even in the presence of a strong incoherent field. The *incoherent* scattered field $\delta\mathbf{E}_{\rm sc}$ originates from the random positions of the scatterers in the ensemble. These two components lead to the coherent and incoherent scattered powers, $P_{\rm coh}$ and $P_{\rm incoh}$. Daily life experience indicates that a gas of atoms or molecules, such as the atmosphere, scatters light efficiently away from the direction of the incoming light beam. However, most of the scattered power is coherent and in the direction of the incoming beam. This suggests a first, and weak criterion for homogenization: $P_{\rm incoh}/P_{\rm coh} \to 0$ when the density of scatterers increases. In this case, the question is therefore whether the effective dielectric constant is enough to describe accurately the propagation of light in the ensemble of scatterers, since coherent light scattering dominates. A second, stronger criterion comes from the observation that pure water or an amorphous glass, which are dense materials with $\rho\lambda^3 \gg 1$, do not scatter light: there is therefore no incoherent scattering ($P_{\rm incoh} = 0$) in this homogenized situation. From these examples, it would seem that the condition $\rho\lambda^3 \gg 1$ leads to homogenization according to at least one of the two criteria described above.

In this work, however, we show theoretically that this condition $\rho\lambda^3 \gg 1$ is not sufficient in the case of dense ensembles of randomly positioned *resonant* scatterers. Our study is motivated by recent experimental developments, which now make it possible to prepare ensembles of resonant scatterers in volumes comparable or smaller than the wavelength of an optical transition, such as ensembles of quantum dots [11,12], clouds of laser-cooled atoms [13,14], or hot atomic vapors in cells with nanometer thickness [15,16]. In particular, we have recently measured both the incoherent [13] and coherent [14] response of a wavelength-sized cold atomic cloud for which the atomic density can be varied. The main result of the present work is the finding that this ensemble of atoms submitted to a near-resonant light field can *never* be homogenized according to both criteria presented above. The situation is all the more striking that, as we have shown in a previous work [17], the effective index of refraction of the cloud can be as large as 2, a value even larger than for many condensed matter systems for which homogenization has been extensively proven to work. We show that the origin of this feature lies in the light-induced dipolar interactions between the atoms that are

very strong when the light is tuned near-resonance. They lead to a collective response of the medium that has to be described in terms of modes rather than in terms of individual atoms.

The paper is organized as follows. We first detail the model used to calculate the coherent and incoherent scattered powers. In Sec. III, we apply our formalism to the far-off resonance case and check that the weak criterion for homogenization applies. Section IV presents the transition from the far-off to the near-resonant case and the fact that a dense cloud of laser-cooled atoms can never be homogenized in the latter regime according to both criteria. We then give a first interpretation in terms of collective modes (Sec. V) and a second one, which considers the cloud as an effective medium described by a dielectric constant (Sec. VI). In Sec. VII, we discuss the influence of correlations in the positions of the scatterers and observe that they lead to a recovery of homogenization according to the two criteria. Finally (Sec.VIII), we show that introducing a nonradiative decay channel also leads to a recovery of homogenization.

II. DESCRIPTION OF THE SYSTEM

We study theoretically the scattering of a plane wave (frequency ω, wave vector $k = \omega/c = 2\pi/\lambda$) from a disordered, wavelength-size cloud of cold atoms, as illustrated in Fig. 1. We idealize the experimental situation of our previous works [13,14] by assimilating the cloud to a parallelepiped with dimensions $V = 4.8\lambda_0 \times 0.6\lambda_0 \times 0.6\lambda_0$, where $\lambda_0 = 780$ nm is the resonance wavelength of the $D2$ transition of rubidium-87 atoms used in the experiment. The atoms are uniformly distributed (spatial density $\rho = N/V$) and modeled as pointlike and identical scatterers characterized by an isotropic polarizability:

$$\alpha(\omega) = \frac{3\pi\Gamma_0/k^3}{\omega_0 - \omega - i\frac{\Gamma_0+\Gamma_{\rm nr}}{2}}, \tag{2}$$

with $\omega_0 = 2\pi c/\lambda_0$ the transition frequency, c the speed of light in vacuum, Γ_0 and $\Gamma_{\rm nr}$, respectively, the radiative and

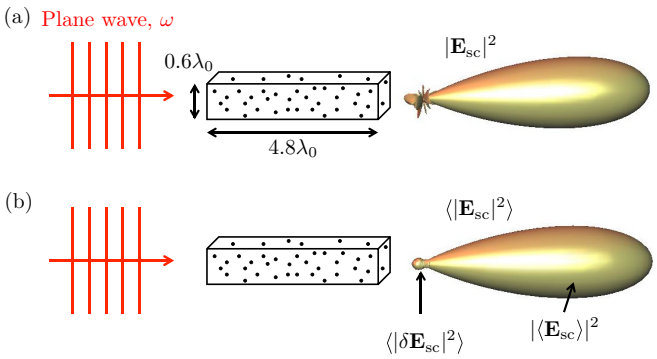

FIG. 1. (a) Scattering pattern $|\mathbf{E}_{\rm sc}|^2$ for a single realization of a cloud of 450 atoms (volume $4.8\lambda_0 \times 0.6\lambda_0 \times 0.6\lambda_0$) illuminated by a plane wave on resonance with the atomic transition ($\omega = \omega_0$). (b) Scattering pattern averaged over 100 realizations of the distribution of atomic positions ($N = 450, \omega = \omega_0$). The speckle structure associated with the incoherent scattering $\langle|\delta\mathbf{E}_{\rm sc}|^2\rangle$ does not show a preferred direction, while the forward direction is dominated by the coherent scattering $|\langle\mathbf{E}_{\rm sc}\rangle|^2$.

nonradiative decay rate ($\Gamma_0 = 2\pi \times 6$ MHz for Rb). When $\Gamma_{\rm nr} = 0$, this polarizability model corresponds to a classical $J = 0 \to J = 1$ atom, where J is the angular momentum.[1] This model can also include nonradiative decay channels ($\Gamma_{\rm nr}$), as would be necessary if we were discussing, e.g., systems of quantum dots. However, unless stated differently, we assume $\Gamma_{\rm nr} = 0$, which is a good model for a cold atomic gas. Finally, the scattering cross section is given by $\sigma_{\rm sc}(\omega) = k^4|\alpha(\omega)|^2/(6\pi)$ [1].

As we discuss dense atomic systems, i.e., $\rho/k^3 \gtrsim 1$, we include the resonant dipole-dipole interactions between the atoms. As explained, e.g., in Refs. [13,14,17], the dipole $\mathbf{p}_j$ of atom j is driven by the laser field and the field radiated by all the other atoms. This approach leads to a set of coupled dipole equations, in steady-state: $\mathbf{p}_j = \epsilon_0\alpha(\mathbf{E}_{{\rm L},j} + \mu_0\omega^2\sum_{i\neq j}[\mathbf{G}(\mathbf{r_i} - \mathbf{r_j})]\mathbf{p}_i)$, with $\mathbf{E}_{{\rm L},j}$ the field of the laser at the position of atom j. Here, the Green's tensor $[\mathbf{G}(\mathbf{r_i} - \mathbf{r_j})]$ describes the resonant dipole-dipole interactions between atoms i and j, including the $1/r$, $1/r^2$, and $1/r^3$ terms. As we deal with a random spatial distribution of atoms, we use the following stochastic procedure: for a given realization of the atomic distribution, we solve the set of coupled equations to get the dipole moment of each atom. We then calculate the scattered electric field $\mathbf{E}_{\rm sc}(\mathbf{r}) = \mu_0\omega^2\sum_i[\mathbf{G}(\mathbf{r} - \mathbf{r_i})]\mathbf{p}_i$ for this particular realization (for more details, see Refs. [13,14,17]). After few hundreds of realizations for which the atomic positions are changed according to a uniform probability distribution, we calculate the scattered field $\mathbf{E}_{\rm sc}$, the coherent, ensemble-average field $\langle\mathbf{E}_{\rm sc}\rangle$, and the incoherent, fluctuating field $\delta\mathbf{E}_{\rm sc} = \mathbf{E}_{\rm sc} - \langle\mathbf{E}_{\rm sc}\rangle$. The ensemble-averaged scattering pattern is then decomposed in its coherent and incoherent parts: $\langle|\mathbf{E}_{\rm sc}|^2\rangle = |\langle\mathbf{E}_{\rm sc}\rangle|^2 + \langle|\delta\mathbf{E}_{\rm sc}|^2\rangle$. The coherent scattering pattern corresponds to the diffraction pattern of a homogeneous object described by an effective dielectric constant and the incoherent scattering pattern is a quasi-isotropic speckle originating from the random positions of the atoms in the cloud (see Fig. 1).

To characterize quantitatively the level of homogenization, we define the integrated scattered powers corresponding, respectively, to the ensemble-averaged fields $|\langle\mathbf{E}_{\rm sc}\rangle|^2$ and $\langle|\delta\mathbf{E}_{\rm sc}|^2\rangle$ evaluated on a spherical surface Σ in the far field:

$$P_{\rm coh} = \frac{\epsilon_0 c}{2}\oint_\Sigma |\langle\mathbf{E}_{\rm sc}\rangle|^2 dS \tag{3}$$

and

$$P_{\rm incoh} = \frac{\epsilon_0 c}{2}\oint_\Sigma \langle|\delta\mathbf{E}_{\rm sc}|^2\rangle dS. \tag{4}$$

The total scattered power is then $P_{\rm tot} = P_{\rm coh} + P_{\rm incoh}$. It does not include the incident field.

III. FAR-OFF RESONANCE LIGHT SCATTERING

Figure 2 presents the coherent and incoherent scattered powers as a function of the number of atoms N inside the fixed volume of the cloud, normalized by the scattered power of a single atom, for different detunings $\Delta = \omega - \omega_0$ of the

[1]Here we neglect the complex internal structure of the rubidium atom used in the experiment.

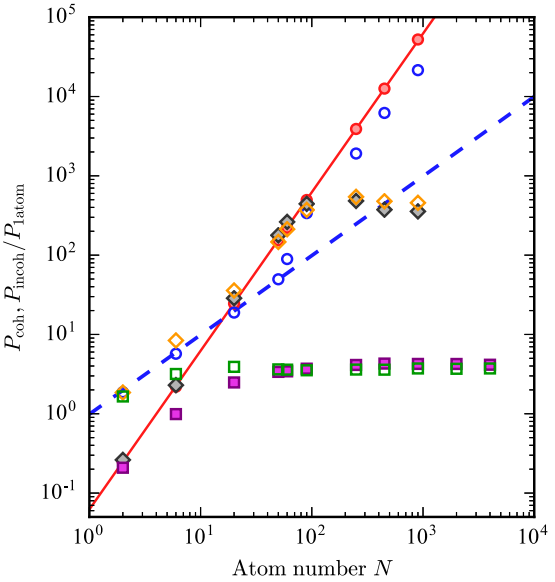

FIG. 2. Coherent (plain symbols) and incoherent (open symbols) scattered powers calculated for a linearly polarized incident plane wave propagating along the long axis of the cloud for various frequency detunings $\Delta = \omega - \omega_0$, as a function of the number of atoms N. All powers are normalized to the power scattered by a single atom at the same detuning. The plain (dashed) line connects the values of the coherent (incoherent) power for $\Delta = -10^4\Gamma_0$. Circles, $\Delta = -500\Gamma_0$; diamonds, $\Delta = -5\Gamma_0$; squares, $\Delta = 0$.

incoming plane wave with respect to the atomic transition. This figure allows us to explore the transition between far-off to near-resonance scattering.

When the laser is very far-off resonance ($\Delta = -10^4\Gamma_0$), we observe the scalings $P_{\rm incoh} \propto N$ and $P_{\rm coh} \propto N^2$. As is recalled in Appendix A, this result is expected as the wavelength-size atomic cloud is in the single scattering regime [18]: the mean free path $\ell_{\rm sc} = 1/[\rho\sigma_{\rm sc}(\omega)] = 3$ m for $N = 450$ atoms is much larger than the size of the atomic cloud. In this regime of large detuning, the weak criterion for homogenization applies, as $P_{\rm incoh}/P_{\rm coh} \propto 1/N \to 0$ when N increases. We note from Fig. 2 that the cloud enters the homogenization regime for $N \gtrsim 20$, i.e., $\rho\lambda^3 > 1$.

The fact that, in the single scattering limit, $P_{\rm incoh} \propto N$ is extensively used to calibrate the number of atoms in a cloud of, e.g., cold atoms in experiments on laser cooling or quantum degenerate gases [19]. It is also common in these experiments to measure the index of refraction of the atomic sample by measuring the coherent optical response of the cloud using, e.g., absorption or phase contrast imaging. This again emphasizes the fact that one can always define an index of refraction (or a dielectric constant) to characterize the coherent response of the cloud, even in the presence of incoherent scattering.

IV. FROM FAR-OFF TO NEAR-RESONANCE SCATTERING: FAILURE OF HOMOGENIZATION

Coming back to Fig. 2, we observe that when the detuning gets closer to resonance, the scaling laws for both the coherent and incoherent scattering as a function of the atom number are strongly modified with respect to the far-off resonance case.

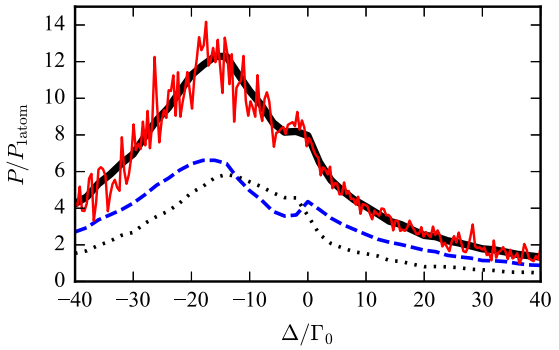

FIG. 3. Total scattered power for a single realization (red line) of a cloud of $N = 450$ atoms, together with the ensemble averaged coherent (dashed blue line), incoherent (dotted black line), and total (thick black line) scattered powers. All quantities are normalized to the power scattered by a single atom at resonance.

When $\Delta = -500\Gamma_0$, the coherent power still follows $P_{\rm coh} \propto N^2$. However, and quite unexpectedly, the incoherent power also features the same N^2 dependence for $N \gtrsim 30$, despite the fact that the cloud still operates in the single-scattering limit ($\ell_{\rm sc} = 3$ mm for $N = 1000$). When the detuning is close to resonance ($\Delta = -5\Gamma_0$), the coherent and incoherent powers are nearly identical for $N \gtrsim 30$ and saturate when $N \gtrsim 100$. Finally, at resonance ($\Delta = 0$), in stark contrast with the off-resonance scattering case, the two powers become rapidly independent of N and saturate to the approximately same value when the number of atoms increases. This saturation of both the incoherent and coherent scattered powers was actually observed in our recent experimental works [13,14], although there we could only measure a fraction of the powers in a given solid angle. As a consequence, as far as the homogenization of the ensemble of atoms is concerned, neither the weak ($P_{\rm incoh}/P_{\rm coh} \to 0$) nor the strong criterion ($P_{\rm incoh} = 0$) apply for detunings in the range $|\Delta/\Gamma_0| \lesssim 500$, although the condition $\rho\lambda^3 \gg 1$ is fulfilled. It thus appears that *a dense cloud of cold atoms can never be homogenized in a broad frequency range around the resonance*! In other words: a dense cloud of cold atoms keeps scattering a lot of incoherent light, and homogenization is reached very far from resonance, and only according to the weak criterion.

Before we give a consistent interpretation of this fact in the next sections, we further explore the resonant case. Figure 1(b) shows the ensemble-averaged scattering pattern of the cloud. We observe that the amplitude of the speckle is very low in the forward direction compared to the coherent scattering. In other directions, incoherent scattering dominates. From the figure, the coherent scattered power seems to dominate the total power. However, as it is scattered in a limited solid angle as opposed to the incoherent power, after integration over all directions it turns out that the coherent and incoherent powers have similar values in our case (see Fig. 2).

Finally, we calculate the powers scattered coherently and incoherently as a function of the detuning of the laser, near the atomic resonance. We plot in Fig. 3 four curves corresponding to (1) the ensemble-averaged coherent scattered light, (2) the

ensemble-averaged incoherent scattered light, (3) the sum of the ensemble-averaged coherent and incoherent scattered light, and (4) the scattered light for a single realization of the distribution of atoms in the cloud. First, we observe that the line shapes are significantly different from a Lorentzian, contrary to what they would be in the single scattering regime. Second, the coherent and incoherent powers exhibit similar shapes, in particular a double structure with a peak for a negative detuning.

All the features presented in this section indicate that the interpretation of scattering as a sequence of individual scattering events breaks down in a broad frequency range around resonance, despite the fact that for all the atom numbers used in this work, the mean-free path ℓ_{sc} is always at least 10 times larger than the cloud largest size, even on resonance. We would otherwise observe a Lorentzian line shape only. This emphasizes that the definition of the mean free path by $\ell_{sc} = 1/[\rho\sigma_{sc}(\omega)]$ is not appropriate to describe the scattering of light in our situation. Instead, the correct length scale is associated with the decay of the field in the medium and is given by $1/(n''k)$, with n'' the imaginary part of the effective refractive index. As n'' reaches values as high as 2 [17], the length scale is 100 nm, smaller than the size of the cloud.

In the next two sections, we interpret the above observations using two different, but complementary points of view.

V. INTERPRETATION IN TERMS OF COLLECTIVE MODES

As discussed by many authors (for recent works, see, e.g., Refs. [17,20–30]), the coupling between atoms resulting from the light-induced dipole-dipole interaction leads to a set of collective modes β of the atomic dipoles. These modes are eigenstates of the set of coupled dipole equations. Each of these $3N$, nonorthogonal modes has its own (complex) eigenfrequency $\tilde{\omega}_\beta = \omega_0 + \Omega_\beta - i\frac{\Gamma_\beta}{2}$, with Ω_β the collective shift and Γ_β the collective decay rate. Some of these modes, featuring $\Gamma_\beta < \Gamma_0$, are subradiant, while others with $\Gamma_\beta > \Gamma_0$ are superradiant. In Ref. [17], we studied in detail the modes corresponding to the situation analyzed here and depicted in Fig. 1. We found that the modes fall in three categories (see Fig. 2 of Ref. [17]). The first one consists of modes with collective linewidth $\Gamma_\beta \approx 2\Gamma_0$ (superradiant) and $\Gamma_\beta \ll \Gamma_0$ (subradiant). These so-called dimer modes are made of pairs of atoms and have large collective frequency shifts $\Omega_\beta \sim \Gamma_0/(kr)^3$, with r the interatomic distance. The second category consists of a few polaritonic modes that have four key features: (i) all atoms have significant contributions to the modes, (ii) they are robust against disorder (i.e., they depend on density and geometry but not on the precise positions of the scatterers), (iii) they are superradiant with $\Gamma_\beta \gtrsim 10\Gamma_0$, and (iv) although representing less than 1% of the total number of modes, we calculated that they contribute for a large (>50%) fraction of the coherent scattering of the cloud. Finally, the last category consists of modes with the excitation delocalized over many atoms, but with no regular spatial structure. They can be super- or subradiant and their frequency shift is on the order of a few Γ_0.

We can now interpret the transition between far-off to near-resonance scattering observed in Fig. 2 in terms of collective modes. First, when the incoming light is very far-detuned, with $|\Delta|$ larger than the largest shift corresponding to the pair of closest atoms in the cloud (see Fig. 2 of Ref. [17]), the light cannot excite any mode. In this regime, the cloud scatters the light as a collection of independent atoms, with the usual scaling laws $P_{incoh} \propto N$ and $P_{coh} \propto N^2$.

When the detuning becomes small enough that dimer modes are excited (see Fig. 2 of Ref. [17]), the incoherent scattering is dominated by the scattering from the superradiant pairs of atoms, which is essentially isotropic for atoms closer than $1/k$. The incoherent scattered power is, therefore, proportional to the number of excited pairs, hence $\propto N^2$. As a consequence, a description in terms of dimer modes naturally leads to a N^2 scaling for the incoherent scattered power. A semiclassical model, presented in Appendix B, predicts a critical number of atoms $N_c \approx 25$, where the transition between scattering by individual atoms to scattering by dimers occurs and is in good agreement with the value observed in Fig. 2. As for the coherent power, we show in Appendix B that it is still dominated by the coherent scattering from individual atoms, with a negligible contribution from the dimers. Therefore, the coherent power varies as N^2 as in the far-off resonance case (see Sec. III and Appendix A).

Finally, when the detuning becomes very close to resonance, many delocalized (nonpolaritonic) modes are excited. Incoherent scattering comes from many of these modes, which have no regular spatial structure. In our intermediate regime $V \sim \lambda^3$, we could not derive any simple scaling law for the incoherent scattering as a function of the atom number. However, qualitatively, the saturation of the *incoherent* power observed in Fig. 2 indicates that, when the number of atoms increases beyond $\rho/k^3 \gtrsim 1$, the product of the number of modes excited in a bandwidth of the order of Γ_0 by the power they radiate has to become independent of the number of atoms. As for the *coherent* scattered power, few polaritonic modes have important contributions. Their collective shifts and widths are mainly set by the geometry of the cloud and hardly depend on the number of atoms [17], leading to a saturation of the coherent power. Finally, we have checked that the saturation of the coherent and incoherent powers at comparable values (see Fig. 2) is a consequence of the particular dimensions of cloud.

VI. INTERPRETATION IN TERMS OF EFFECTIVE MEDIUM

In this second approach, we forget about the discrete atomic distribution and consider instead the cloud as an effective homogeneous medium with a dielectric constant $\epsilon_{eff}(\omega) = \epsilon'_{eff}(\omega) + i\epsilon''_{eff}(\omega)$. In this *macroscopic* description, the absorbed power is given by the imaginary part of the dielectric constant and the macroscopic, ensemble-averaged field $\langle \mathbf{E}(\mathbf{r}) \rangle$ inside the medium [1]:

$$P_{abs}^{macro} = \int_V \frac{1}{2}\mathrm{Re}[\langle \mathbf{J} \rangle \cdot \langle \mathbf{E}^* \rangle]\, dV = \frac{\omega}{2}\epsilon_0\epsilon''_{eff}(\omega) \int_V |\langle \mathbf{E}(\mathbf{r}) \rangle|^2\, dV, \quad (5)$$

with $\langle \mathbf{J} \rangle = -i\omega\epsilon_0[\epsilon_{\text{eff}}(\omega) - 1]\langle \mathbf{E} \rangle$. A detailed balance derived in Appendix C shows that the total power P_{ext} taken from the incident field is the sum of the power absorbed by the cloud and of the scattered power $P_{\text{sc}}^{\text{macro}}$, i.e., $P_{\text{ext}} = P_{\text{abs}}^{\text{macro}} + P_{\text{sc}}^{\text{macro}}$. Now, in a *microscopic* description, this same power P_{ext} is also the sum of the coherent and incoherent scattered powers, defined after ensemble averaging by Eqs. (3) and (4): $P_{\text{ext}} = P_{\text{coh}} + P_{\text{incoh}}$.[2] Finally, the coherent scattered power defined by Eq. (3) is the power scattered in the macroscopic approach, $P_{\text{coh}} = P_{\text{sc}}^{\text{macro}}$, leading to the identification of the absorbed power $P_{\text{abs}}^{\text{macro}}$ with the power P_{incoh} incoherently scattered by the cloud, i.e.,

$$\frac{\epsilon_0 c}{2} \oint_\Sigma \langle |\delta \mathbf{E}_{\text{sc}}|^2 \rangle \, dS = \frac{\omega}{2} \epsilon_0 \epsilon''_{\text{eff}}(\omega) \int_V |\langle \mathbf{E}(\mathbf{r}) \rangle|^2 \, dV. \tag{6}$$

As a consequence, the homogenization criteria $P_{\text{incoh}} = 0$ requires that the imaginary part of the dielectric constant is negligible.[3]

We can now discuss the behavior of the coherent and incoherent scattered powers as a function of the detuning shown in Fig. 3. As we studied in Ref. [17], once we know the effective dielectric constant $\epsilon_{\text{eff}}(\omega)$, we can calculate the electric field inside the cloud considered as a continuous medium. We find resonances for certain values of the frequency ω, precisely corresponding to the polaritonic modes. When hitting a resonance, the electric field $\langle \mathbf{E} \rangle$ inside the medium is large. Consequently, the scattered field, and therefore the coherent power, is large as well. The variation of the coherent scattered power shown in Fig. 3 thus reflects the mode structure of the effective homogeneous particle equivalent to the cloud. We have, for example, checked numerically that the frequency corresponding to the maximum of the broad peak on the red side of the resonance is proportional to the length of the cloud, a signature of a shape resonance in an object of finite size.

The fact that the incoherent and coherent scattered powers show similar behavior as a function of ω is a direct consequence of Eq. (6): if $\epsilon''_{\text{eff}}(\omega)$ were independent of ω, then the two powers would vary identically with ω. As we showed in Ref. [17], $\epsilon''_{\text{eff}}(\omega)$ is in fact a broad, resonant function, and the incoherent scattered power combines the shape resonance of $\langle \mathbf{E} \rangle$ with the resonant behavior of $\epsilon''_{\text{eff}}(\omega)$.

Finally, we can also understand why the coherent and incoherent scattered powers saturate when the number of atoms increases. For large atom numbers, the cloud behaves like a sharp object. The coherent scattering corresponds to the diffraction pattern of this object [3,31] and is only dependent on its shape.[4] To understand why the incoherent power also saturates at large atom numbers, we rely on the expression of the coherent power scattered by an object of volume V and dielectric constant $\epsilon_{\text{eff}}(\omega)$ [3]:

$$P_{\text{coh}} = \frac{\epsilon_0 \omega^4}{32\pi^2 c^3} |\epsilon_{\text{eff}}(\omega) - 1|^2 \left| \int_{4\pi} d\Omega \, \mathbf{e}_r \times \int_V d^3\mathbf{r}' \langle \mathbf{E}(\mathbf{r}') \rangle \, e^{-i\mathbf{k}\cdot\mathbf{r}'} \right|^2, \tag{7}$$

with $\mathbf{e}_r$ the unit vector in a given scattering direction. If the coherent scattered power saturates for large atom numbers, as it should based on the diffraction argument above, this formula indicates that the coherent field inside the object and the dielectric constant must saturate. Therefore, according to Eq. (6) the incoherent power must saturate as well.

VII. INFLUENCE OF THE CORRELATIONS IN THE POSITIONS OF THE ATOMS

The impossibility to reach homogenization for an ensemble of cold atoms presented in Fig. 2 makes us wonder if there exists any resonant system that can reach the homogenization regime. In this section, we show that a way to make this ensemble of scatterers homogenized consists in introducing spatial correlations in the positions of the atoms to reduce the fluctuations of the spatial distribution [4,8,9]. We are guided here by the well-known fact that a pure liquid scatters less light than a gas, although being much denser: the presence of position correlations in the liquid inhibits incoherent scattering. Another situation is the transparency of the cornea, which is due to spatial correlations [32].

Here we implement spatial correlations by introducing a spherical exclusion volume with diameter d around each scatterer.[5] This diameter sets the minimum distance between nearest-neighbor scatterers. Figure 4 presents the coherent and incoherent scattered powers as a function of the diameter d of the exclusion volume for $N = 100$ and various detunings. We observe that for Δ ranging from $-10^4\Gamma_0$ to $\sim -10\Gamma_0$, incoherent light scattering is reduced by introducing spatial order in the system, while the coherent scattering is weakly affected. As a consequence, this procedure leads to homogenization according to the stringent criterion $P_{\text{incoh}} = 0$. Qualitatively, this suppression comes from the fact that the exclusion volume thwarts the formation of dimer modes.

Closer to resonance, the behavior is more complex. For detunings in the range $-5 \leqslant \Delta/\Gamma_0 < 0$, we observe an increase of the coherent power, while the incoherent decreases. At resonance ($\Delta = 0$), coherent power still increases with d, while the incoherent power remains approximatively constant. These findings seem to indicate that the spatial correlations lead to at least the weak homogenization criterion, with a decrease of the ratio $P_{\text{incoh}}/P_{\text{coh}}$. We could not explore exclusion diameters larger than $0.2\lambda_0$, while maintaining the

[2] We have assumed here that the atoms are elastic scatterers that do not absorb light as, e.g., particles in China ink would.

[3] Care must be taken that the fact that we can describe the incoherent power by the imaginary part of the effective (i.e., ensemble-averaged) dielectric constant does not imply that the incoherent field itself is described by an effective dielectric constant.

[4] As an example, the scattering cross section of an homogeneous particle with a size larger than the wavelength of the scattered light is twice the geometrical cross section perpendicular to the incoming wave direction and is therefore independent of the number of atoms in the particle.

[5] In this calculation, the number of atoms N is kept constant. If for a given distribution we find that two atoms are distant by less than d, we draw a new configuration with the same number of atoms.

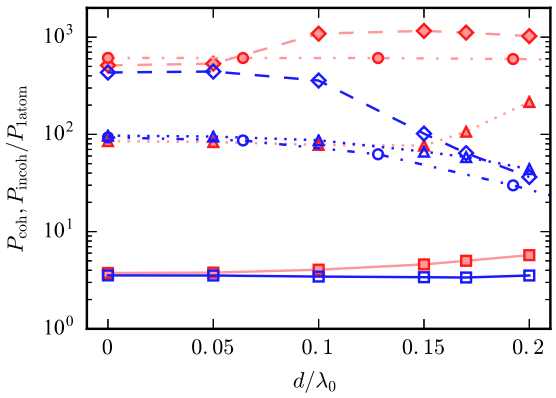

FIG. 4. Influence of position correlations on incoherent (blue open symbols) and coherent (red plain symbols) scattering calculated for $N = 100$ as a function of the diameter d of the spherical exclusion volume around each atom, for various detunings Δ. Circles, $\Delta = -10^4\Gamma_0$; diamonds, $\Delta = -5\Gamma_0$; triangles, $\Delta = -2\Gamma_0$; squares, $\Delta = 0$.

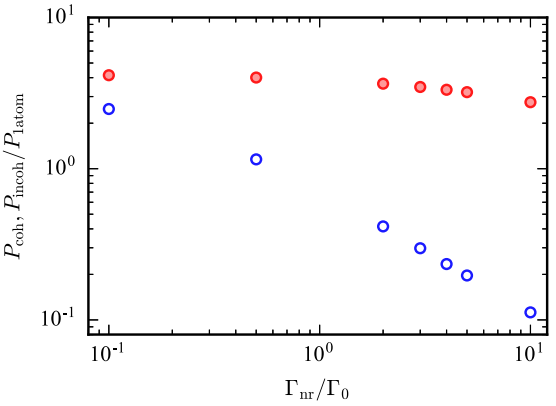

FIG. 5. Coherent (red plain circles) and incoherent (blue open circles) scattered powers on resonance ($\Delta = 0$) for $N = 450$ atoms as a function of the non-radiative decay rate $\Gamma_{\rm nr}$. All powers are normalized by the power scattered by a single atom at resonance.

number of atoms constant,[6] and therefore could not check the point when the stringent criterion starts to be valid.

VIII. EFFECT OF NONRADIATIVE LOSSES ON NEAR-RESONANCE LIGHT SCATTERING

In this last section, we discuss the influence of nonradiative losses on light scattering. We know that, for example, a suspension of nonresonant absorbing particles, such as a droplet of China ink consisting of a suspension of colloidal carbon nanoparticles, does not scatter light if the absorption cross section is much larger than the scattering cross section of each particle. In this case, all the energy gets absorbed by the particles, converted into heat, and scattering can be neglected. Guided by this example of a nonresonant situation, we introduce here nonradiative losses and study if homogenization according to the strong criterion ($P_{\rm incoh} = 0$) is reached in the resonant case as well. Although this procedure would not apply to a cold atomic ensemble, it would be relevant for ensembles of, e.g., molecules or quantum dots coupled to phonons.

We report in Fig. 5 the coherent and incoherent powers calculated for resonant light scattering for different values of the ratio of the nonradiative loss rate $\Gamma_{\rm nr}$ relative to the radiative loss rate Γ_0. We observe that as the amount of nonradiative losses increases, the incoherent power gets significantly reduced, whereas the coherent power is only slightly affected.

This observation can be understood by using the collective mode picture. By introducing nonradiative losses characterized by the rate $\Gamma_{\rm nr}$, the only change to the (complex) eigenfrequency of a collective eigenmode β is to replace its value $\tilde{\omega}_\beta = \omega_0 + \Omega_\beta - i\frac{\Gamma_\beta}{2}$ by $\tilde{\omega}_\beta - i\frac{\Gamma_{\rm nr}}{2}$. As a consequence, the modes with radiative decay rates $\Gamma_\beta < \Gamma_{\rm nr}$ damp in a time $1/\Gamma_{\rm nr}$, irrespective of their radiative damping rate. Therefore, when $\Gamma_{\rm nr} > \Gamma_0$, the subradiant modes ($\Gamma_\beta < \Gamma_0$) decay nonradiatively very quickly and therefore hardly contribute to the scattering in steady state. As they are in particular responsible for the incoherent scattering, this one is suppressed. By contrast, light scattered by a polaritonic (superradiant) mode is not affected by the nonradiative decay as long as $\Gamma_\beta > \Gamma_{\rm nr} > \Gamma_0$. These polaritonic modes lead to coherent scattering. Finally, when the radiative decay rate of the most superradiant mode gets smaller than $\Gamma_{\rm nr}$, even the coherent scattering is suppressed. Therefore, the introduction of nonradiative losses appears as an efficient way to achieve homogenization in the sense of suppressing incoherent light scattering.

IX. CONCLUSION

As a conclusion, we have studied theoretically the concept of homogenization in optics using an ensemble of resonant scatterers dense enough for the usual condition for homogenization, viz. $\rho\lambda^3 \gg 1$, to be reached. We have introduced two criteria to define the homogenization regime in terms of incoherent and coherent scattered powers. When the excitation field is tuned very far from the resonance of the scatterers, we recovered the well-known scaling laws as a function of the atom number N, leading to a suppression of the ratio $P_{\rm incoh}/P_{\rm coh}$ at large N. However, when excited in a broad frequency range around the resonance, we observed that none of the criteria for homogenization apply, meaning that the condition $\rho\lambda^3 \gg 1$ is not sufficient to characterize the homogenized regime. We interpreted this result as an effect of the dipole-dipole interactions between the atoms, which implies a description of scattering in terms of collective modes rather than as a sequence of individual scattering events. Finally, we showed that, although homogenization can never be reached for a dense ensemble of randomly positioned laser-cooled atoms, it becomes possible if one introduces spatial correlations in the positions of the atoms or nonradiative losses, such as would be the case for organic molecules or quantum dots coupled to a phonon bath.

[6]When increasing the diameter d, the probability to find an exclusion volume with only one atom becomes too small.

ACKNOWLEDGMENTS

We thank R. Carminati for fruitful discussions. We acknowledge support from the French National Research Agency (ANR) as part of the "Investissements d'Avenir" program (Labex PALM, ANR-10-LABX-0039), and Région Ile-de-France (LISCOLEM project). N.J.S. is supported by Triangle de la Physique (COLISCINA project) and Université Paris-Sud. J.-J.G. acknowledges support from Institut Universitaire de France and the SAFRAN-IOGS chair on Ultimate Photonics.

APPENDIX A: SCATTERING BY AN ENSEMBLE OF ATOMS IN THE SINGLE-SCATTERING LIMIT

In this appendix, we summarize textbook arguments about scattering from ensemble of scatterers in the single-scattering limit, valid when the mean-free path $\ell_{sc} = 1/[\rho\sigma_{sc}(\omega)]$ is much larger than the size of the ensemble. The power scattered at a distance r in the direction $\mathbf{k}$ by the ensemble of N atoms placed at positions r_j is then proportional to

$$|\mathbf{E}_{sc}(\mathbf{k})|^2 = |\mathbf{E}_{0,sc}(\mathbf{k})|^2\, S(\mathbf{k}-\mathbf{k}_L), \tag{A1}$$

where $\mathbf{k}_L$ is the wave vector of the incident plane wave, $\mathbf{E}_{0,sc}(\mathbf{k})$ the field scattered by a single atom, and

$$S(\mathbf{q}) = \left|\sum_{j=1}^{N} e^{i\mathbf{q}\cdot\mathbf{r}_j}\right|^2 \tag{A2}$$

the structure factor of the cloud. The ensemble-average power in the direction $\mathbf{k} = \mathbf{k}_L + \mathbf{q}$ is then proportional to $\langle S(\mathbf{q})\rangle$ and, thus,

$$\langle|\mathbf{E}_{sc}(\mathbf{k})|^2\rangle \propto N(1 - \langle e^{i\mathbf{q}\cdot(\mathbf{r}-\mathbf{r}')}\rangle) + N^2\langle e^{i\mathbf{q}\cdot(\mathbf{r}-\mathbf{r}')}\rangle. \tag{A3}$$

Here, the average phase factor is given by

$$\langle e^{i\mathbf{q}\cdot(\mathbf{r}-\mathbf{r}')}\rangle = \int_V d^3\mathbf{r}d^3\mathbf{r}'\, P(\mathbf{r},\mathbf{r}')e^{i\mathbf{q}\cdot(\mathbf{r}-\mathbf{r}')}, \tag{A4}$$

with $P(\mathbf{r},\mathbf{r}')$ the joint probability distribution to find a particle at position $\mathbf{r}$ and $\mathbf{r}'$. When the positions are not correlated, $P(\mathbf{r},\mathbf{r}') = \rho(\mathbf{r})\rho(\mathbf{r}')/N^2$, with $\rho(\mathbf{r})$ the spatial density distribution, and the term $\langle e^{i\mathbf{q}\cdot(\mathbf{r}-\mathbf{r}')}\rangle$ is the diffraction pattern of the cloud:

$$\langle e^{i\mathbf{q}\cdot(\mathbf{r}-\mathbf{r}')}\rangle = \left|\frac{1}{N}\int_V d^3\mathbf{r}\rho(\mathbf{r})e^{i\mathbf{q}\cdot\mathbf{r}}\right|^2. \tag{A5}$$

The N^2 term in Eq. (A3) is the coherent component and dominates in the solid angle corresponding to diffraction. In the other directions, the power is proportional to N and corresponds to the incoherent scattering. It is almost isotropic.

APPENDIX B: CONTRIBUTION OF THE DIMER MODES TO INCOHERENT SCATTERING IN THE INTERMEDIATE DETUNING REGIME

Here we derive a semiclassical model to calculate the critical number of atoms N_c where the transition between scattering by individual atoms to scattering by dimers occurs (Sec. V). This model is inspired by the one used to calculate the rate of light-assisted collisions in cold atomic samples [33,34].

As explained in Sec. V, in the intermediate detuning regime the incoherent scattering is due to the superradiant pairs of atoms. We first note that when two atoms are separated by $r \ll 1/k$, their interaction energy is dominated by the dipolar (near-field) term: $U(r) \sim \hbar\Gamma_0/(kr)^3$. To estimate the incoherent scattered power, we start by calculating the number of excited pairs as follows: for a given detuning $|\Delta|$, the light is resonant with the excitation of a pair of atoms located at a relative distance r_{ex} such that $|\Delta| \sim \Gamma_0/(kr_{ex})^3$. The number of excited dimers is then the product of the atom number N with the number of atoms in a shell of radius r_{ex},$(N/V)4\pi r_{ex}^2\Delta r$, with V the cloud volume, N the atom number, and Δr the thickness of the shell. The latter one is determined by writing that the collective width $2\Gamma_0$ of a superradiant pair is $U'(r_{ex})\Delta r/\hbar = 3\Gamma_0/(kr_{ex})^3(\Delta r/r_{ex})$. As a consequence, assuming that approximatively half the dimers are superradiant, the number of superradiant pairs is $N_p \sim (N^2/2)[8\pi/(3k^3V)](\Gamma_0/\Delta)^2$. The power scattered by a superradiant pair (decay rate $2\Gamma_0$, saturation intensity of the dimer transition $2I_{sat}$, with I_{sat} the atomic saturation intensity) irradiated by a light with intensity $I \ll I_{sat}$ is $P_{dimer} = \hbar\omega_0(2\Gamma_0)I/(4I_{sat})$. Finally, the power scattered by a single atom irradiated by the same light detuned by $|\Delta|$ with respect to the atomic transition is $P_0 \approx \hbar\omega_0\Gamma_0 I/(2I_{sat})(\Gamma_0/2\Delta)^2$. Combining the expressions above, we find the ratio of the total incoherent power scattered by the cloud to the power scattered by a single atom: $P_{incoh}/P_0 \sim N^2[16\pi/(3k^3V)]$. The critical number of atoms N_c, where the transition between scattering by individual atoms to scattering by dimers occurs, is thus $N_c \sim 3k^3V/(16\pi)$. The transition point is thus predicted to be independent of the detuning, in agreement with numerical calculations performed for various detunings. Also, for our parameters, $N_c \approx 25$, in good agreement with the value observed in Fig. 2, considering the simplicity of the model.

We now calculate the coherent power P_{coh}^{dim} scattered by the dimers and compare it to the coherent scattering due to individual atoms P_{coh}^{at}. This latter one is given by $P_{coh}^{at} = N^2P_0\,\Omega/(4\pi)$, as for the intermediate detunings, the cloud is still in the single scattering regime. Here, $\Omega/(4\pi)$ is the solid angle of the diffraction pattern. The power coherently scattered by the dimers is $P_{coh}^{dim} = N_p^2 P_{dimer}\,\Omega/(4\pi)$ as the dimers are spread in a dilute way in the same volume as the atoms. Finally, we get $P_{coh}^{dim}/P_{coh}^{at} = [8\pi/(3k^3V)]^2N^2(\Gamma_0/\Delta)^2$. For $N \lesssim 500$ and $|\Delta|/\Gamma_0 = 100$–500, $P_{coh}^{dim}/P_{coh}^{at} \ll 1$, thus making the contribution of the dimers to coherent scattering negligible.

APPENDIX C: DERIVATION OF THE DETAILED BALANCE USED IN SEC. VI

Here we give an explicit derivation of Eq. (6). We consider the ensemble (volume V) of discrete atoms and a spherical surface Σ with a radius $r \gg 1/k$. The conservation of energy in steady-state state tells us that the flux of the time-averaged Poyting vector through Σ compensates for the time-averaged power dissipated by the current in the volume V:

$$\frac{1}{2}\mathrm{Re}\left[\oint_\Sigma \mathbf{E}\times\mathbf{H}^*\cdot d\mathbf{S} + \int_V \mathbf{J}\cdot\mathbf{E}^*\, dV\right] = 0, \tag{C1}$$

with $\mathbf{H} = \mathbf{B}/\mu_0$ (non magnetic medium) and $\mathbf{J}$ the current density in the ensemble. This expression is valid in a microscopic model. We now decompose the fields into the incoming component, the coherent scattered component and the incoherent part: $\mathbf{E} = \mathbf{E}_\mathrm{i} + \langle \mathbf{E}_\mathrm{sc} \rangle + \delta\mathbf{E}_\mathrm{sc}$ and $\mathbf{H} = \mathbf{H}_\mathrm{i} + \langle \mathbf{H}_\mathrm{sc} \rangle + \delta\mathbf{H}_\mathrm{sc}$, with $\langle . \rangle$ denoting an ensemble average. We also decompose the current density into an ensemble average and a fluctuating part: $\mathbf{J} = \langle \mathbf{J} \rangle + \delta\mathbf{J}$. As $\oint_\Sigma \mathbf{E}_\mathrm{i} \times \mathbf{H}_\mathrm{i}^* \cdot d\mathbf{S} = 0$, the extinction power P_ext taken from the incident field is, after expansion and ensemble average,

$$\begin{aligned} P_\mathrm{ext} &= -\frac{1}{2}\mathrm{Re}\left[\oint_\Sigma (\mathbf{E}_\mathrm{i} \times \langle \mathbf{H}_\mathrm{sc}^* \rangle + \langle \mathbf{E}_\mathrm{sc} \rangle \times \mathbf{H}_\mathrm{i}^*) \cdot d\mathbf{S} \right] \\ &= -\frac{1}{2}\mathrm{Re}\left[\oint_\Sigma \langle \mathbf{E}_\mathrm{sc} \rangle \times \langle \mathbf{H}_\mathrm{sc}^* \rangle \cdot d\mathbf{S} + \oint_\Sigma \langle \delta\mathbf{E}_\mathrm{sc} \times \delta\mathbf{H}_\mathrm{sc}^* \rangle \cdot d\mathbf{S} \right. \\ &\quad \left. + \int_V \langle \mathbf{J} \rangle \cdot \langle \mathbf{E}^* \rangle \, dV + \int_V \langle \delta\mathbf{J} \cdot \delta\mathbf{E}^* \rangle \, dV \right], \end{aligned} \tag{C2}$$

with $\langle \mathbf{E} \rangle = \mathbf{E}_\mathrm{i} + \langle \mathbf{E}_\mathrm{sc} \rangle$. For a cloud of cold atoms, no energy is dissipated in the medium as all incident power is rescattered. Therefore,

$$\int_V \langle \mathbf{J} \cdot \mathbf{E}^* \rangle \, dV = \int_V \langle \delta\mathbf{J} \cdot \delta\mathbf{E}^* \rangle \, dV + \int_V \langle \mathbf{J} \rangle \cdot \langle \mathbf{E}^* \rangle \, dV = 0. \tag{C3}$$

In this case, $P_\mathrm{ext} = P_\mathrm{coh} + P_\mathrm{incoh}$ using the definitions of the coherent [Eq. (3)] and incoherent [Eq. (4)] scattered powers.

Now, for the homogeneous medium with an effective permittivity equivalent to the ensemble of atoms, $\delta\mathbf{J} = \mathbf{0}$, $\delta\mathbf{E} = \delta\mathbf{E}_\mathrm{sc} = \mathbf{0}$, and $\delta\mathbf{H}_\mathrm{sc} = \mathbf{0}$, and Eq. (C2) yields

$$\begin{aligned} P_\mathrm{ext} &= -\frac{1}{2}\mathrm{Re}\left[\oint_\Sigma (\mathbf{E}_\mathrm{i} \times \langle \mathbf{H}_\mathrm{sc}^* \rangle + \langle \mathbf{E}_\mathrm{sc} \rangle \times \mathbf{H}_\mathrm{i}^*) \cdot d\mathbf{S} \right] \\ &= \frac{1}{2}\mathrm{Re}\left[\oint_\Sigma \langle \mathbf{E}_\mathrm{sc} \rangle \times \langle \mathbf{H}_\mathrm{sc}^* \rangle \cdot d\mathbf{S} + \int_V \langle \mathbf{J} \rangle \cdot \langle \mathbf{E}^* \rangle \, dV \right]. \end{aligned} \tag{C4}$$

As $P_\mathrm{coh} = \frac{1}{2}\mathrm{Re}[\oint_\Sigma \langle \mathbf{E}_\mathrm{sc} \rangle \times \langle \mathbf{H}_\mathrm{sc}^* \rangle \cdot d\mathbf{S}]$, we get by identification

$$P_\mathrm{incoh} = \frac{1}{2}\mathrm{Re}\left[\int_V \langle \mathbf{J} \rangle \cdot \langle \mathbf{E}^* \rangle \, dV \right], \tag{C5}$$

or equivalently, $P_\mathrm{incoh} = P_\mathrm{abs}^\mathrm{macro}$.

[1] D. J. Jackson, *Classical Electrodynamics* (John Wiley and Sons, New York, 1998).

[2] N. W. Ashcroft and N. D. Mermin, *Solid State Physics* (Brooks Cole, Boston, 1976).

[3] A. Zangwill, *Modern Electrodynamics* (Cambridge University Press, Cambridge, UK, 2012).

[4] U. Frisch, in *Probabilistic Methods in Applied Mathematics*, edited by A. A. Bharuch-Reid (Academic Press, New York, 1968), Vols. I and II.

[5] J. C. Maxwell-Garnett, Colors in metal glasses and in metallic films, Phil. Trans. R. Soc. London A **203**, 385 (1904).

[6] D. A. G. Bruggeman, Berechnung verschiedener physikalischer Konstanten von heterogenen Substanzen. I. Dielektrizitätskonstanten und Leitfähigkeiten der Mischkörper aus isotropen Substanzen, Ann. Phys. **416**, 636 (1935).

[7] P. Sheng, *Introduction to Wave Scattering, Localization, and Mesoscopic Phenomena* (Academic Press, New York, 1995).

[8] A. Lagendijk and B. van Tiggelen, Resonant multiple scattering of light, Phys. Rep. **270**, 143 (1996).

[9] S. Durant, O. Calvo-Perez, N. Vukadinovic, and J.-J. Greffet, Light scattering by a random distribution of particles embedded in absorbing media: Diagrammatic expansion of the extinction coefficient, J. Opt. Soc. Am. A **24**, 9 (2007).

[10] P. Mallet, C. A. Guérin, and A. Sentenac, Maxwell-Garnett Mixing Rule in the Presence of Multiple Scattering: Derivation and Accuracy, Phys. Rev. B **72**, 014205 (2005).

[11] L. Novotny and B. Hecht, *Principles of Nano-Optics* (Cambridge University Press, Cambridge, 2006).

[12] C. Belacel *et al.*, Controlling spontaneous emission with plasmonic optical patch antennas, NanoLetters **13**, 1516 (2013).

[13] J. Pellegrino, R. Bourgain, S. Jennewein, Y. R. P. Sortais, A. Browaeys, S. D. Jenkins, and J. Ruostekoski, Observation of Suppression of Light Scattering Induced by Dipole-Dipole Interactions in a Cold-Atom Ensemble, Phys. Rev. Lett. **113**, 133602 (2014).

[14] S. Jennewein, M. Besbes, N. J. Schilder, S. D. Jenkins, C. Sauvan, J. Ruostekoski, J.-J. Greffet, Y. R. P. Sortais, and A. Browaeys, Coherent Scattering of Near-Resonant Light by a Dense Microscopic Cold Atomic Cloud, Phys. Rev. Lett. **116**, 233601 (2016).

[15] J. Keaveney, A. Sargsyan, U. Krohn, I. G. Hughes, D. Sarkisyan, and C. S. Adams, Cooperative Lamb Shift in an Atomic Vapor Layer of Nanometer Thickness, Phys. Rev. Lett. **108**, 173601 (2012).

[16] J. Keaveney, I. G. Hughes, A. Sargsyan, D. Sarkisyan, and C. S. Adams, Maximal Refraction and Superluminal Propagation in a Gaseous Nanolayer, Phys. Rev. Lett. **109**, 233001 (2012).

[17] N. J. Schilder, C. Sauvan, J.-P. Hugonin, S. Jennewein, Y. R. P. Sortais, A. Browaeys, and J.-J. Greffet, Role of polaritonic modes on light scattering from a dense cloud of atoms, Phys. Rev. A **93**, 063835 (2016).

[18] F. S. Crawford, *Waves: Berkeley Physics Course* (McGraw-Hill, New York, 1968), Vol. 3, p. 559.

[19] W. Ketterle, D. S. Durfee, and D. M. Stamper-Kurn, Making, probing and understanding Bose-Einstein condensates, in *Proceedings of the International School of Physics Enrico Fermi, Course CXL*, edited by M. Inguscio, S. Stringari, and C. E. Wieman (IOS Press, Amsterdam, 1999).

[20] J. Ruostekoski and J. Javanainen, Quantum field theory of cooperative atom response: Low light intensity, Phys. Rev. A **55**, 513 (1997).

[21] A. A. Svidzinsky, J.-T. Chang, and M. O. Scully, Cooperative spontaneous emission of N atoms: Many-body eigenstates, the

effect of virtual Lamb shift processes, and analogy with radiation of N classical oscillators, Phys. Rev. A **81**, 053821 (2010).

[22] L. Chomaz, L. Corman, T. Yefsah, R. Desbuquois, and J. Dalibard, Absorption imaging of a quasi-two-dimensional gas: A multiple scattering analysis, New J. Phys. **14**, 055001 (2012).

[23] S. Balik, A. L. Win, M. D. Havey, I. M. Sokolov, and D. V. Kupriyanov, Near-resonance light scattering from a high-density ultracold atomic ^{87}Rb gas, Phys. Rev. A **87**, 053817 (2013).

[24] Y. Li, J. Evers, W. Feng, and S.-Y. Zhu, Spectrum of collective spontaneous emission beyond the rotating-wave approximation, Phys. Rev. A **87**, 053837 (2013).

[25] L. Bellando, A. Gero, E. Akkermans, and R. Kaiser, Cooperative effects and disorder: A scaling analysis of the spectrum of the effective atomic Hamiltonian, Phys. Rev. A **90**, 063822 (2014).

[26] R. J. Bettles, S. A. Gardiner, and C. S. Adams, Cooperative ordering in lattices of interacting two-level dipoles, Phys. Rev. A **92**, 063822 (2015).

[27] R. J. Bettles, S. A. Gardiner, and C. S. Adams, Cooperative eigenmodes and scattering in one-dimensional atomic arrays, Phys. Rev. A **94**, 043844 (2016).

[28] S. D. Jenkins, J. Ruostekoski, J. Javanainen, S. Jennewein, R. Bourgain, J. Pellegrino, Y. R. P. Sortais, and A. Browaeys, Collective resonance fluorescence in small and dense atom clouds: Comparison between theory and experiment, Phys. Rev. A **94**, 023842 (2016).

[29] J. Javanainen and J. Ruostekoski, Light propagation beyond the mean-field theory of standard optics, Opt. Express **24**, 993 (2016).

[30] J. Javanainen, J. Ruostekoski, Y. Li, and S.-M. Yoo, Shifts of a Resonance Line in a Dense Atomic Sample, Phys. Rev. Lett. **112**, 113603 (2014).

[31] C. F. Bohren and D. R. Huffman, *Absorption and Scattering of Light by Small Particles* (John Wiley & Sons, New York, 1983).

[32] R. W. Hart and R. A. Farrell, Light scattering in the cornea, J. Opt. Soc. Am. **59**, 766 (1969).

[33] A. Gallagher and D. E. Pritchard, Exoergic Collisions of Cold Na*-Na, Phys. Rev. Lett. **63**, 957 (1989).

[34] J. Weiner, V. S. Bagnato, S. Zilio, and P. S. Julienne, Experiments and theory in cold and ultracold collisions, Rev. Mod. Phys. **71**, 1 (1999).